ORIGINAL

Texture analysis of sonographic muscle images can distinguish myopathic conditions

Hiroyuki Nodera[1,5], Kazuki Sogawa[3], Naoko Takamatsu[1], Shuji Hashiguchi[2], Miho Saito[2], Atsuko Mori[1, 4], Yusuke Osaki[1], Yuishin Izumi[1], and Ryuji Kaji[1]

[1]Department of Neurology, Tokushima University, Tokushima, Japan, [2]Tokushima Hospital, Tokushima, Japan, [3]Faculty of Medicine, Tokushima University, Tokushima, Japan, [4]Itsuki Hospital, Tokushima, Japan, [5]Department of Neurology, Kanazawa Medical University, Ishikawa, Japan

Abstract : Given the recent technological advent of muscle ultrasound (US), classification of various myopathic conditions could be possible, especially by mathematical analysis of muscular fine structure called texture analysis. We prospectively enrolled patients with three neuromuscular conditions and their lower leg US images were quantitatively analyzed by texture analysis and machine learning methodology in the following subjects : Inclusion body myositis (IBM) [N=11] ; myotonic dystrophy type 1 (DM1) [N=19] ; polymyositis/dermatomyositis (PM-DM) [N=21]. Although three-group analysis achieved up to 58.8% accuracy, two-group analysis of IBM plus PM-DM versus DM1 showed 78.4% accuracy. Despite the small number of subjects, texture analysis of muscle US followed by machine learning might be expected to be useful in identifying myopathic conditions. J. Med. Invest. 66 : 237-240, August, 2019

Keywords **:** *myopathy, texture analysis, muscle ultrasound, machine learning*

INTRODUCTION

Imaging study of skeletal muscles has been clinically utilized in various neuromuscular conditions. Muscle ultrasound (US) has advantages of its low cost, portability, and relative lack of contraindications in comparison to muscle MRI. Because muscle US detects abnormal echo intensities (EIs) as well as abnormal size in various myopathic conditions, characteristic localization of abnormal EIs has been utilized as diagnostic clues in myopathies.

Muscle EIs can be assessed by a number of methods. The most commonly used is the mean EI in a particular region of interest (ROI). Normal muscle tissues have low EIs and surrounding fascial tissues have high EIs. In myopathic conditions, muscle EIs tend to increase, reflecting lipid replacement and fibrosis. Another method is a histogram that shows the overall distribution of the tissue by observing the shape of the histogram (e.g., skewness and kurtosis). This histogram-based characteristics are calculated by counting the EIs from each pixel, without considering the relative relationships of adjacent pixels. By contrast, mathematical calculation of relative relationships of adjacent pixels is called texture analysis. (1, 2) Texture analysis gives us information about the spatial arrangement of EIs in an image. Sogawa and colleagues reported that US-texture analysis can classify leg muscles with neuropathic conditions and myopathic ones. (3) However, data are lacking whether muscle echo texture has characteristic abnormalities in different myopathic diseases. Thus, the aim of this study was to assess whether muscle echo texture can differentiate myopathic diseases.

METHODS

Subjects

Three groups were recruited and prospectively assessed : (1) patients with sporadic inclusion body myositis (s-IBM) who met clinical-pathologically defined IBM or clinically defined IBM criteria based on guidelines from the European Neuromuscular Center (ENMC), with no family history of related conditions ; (2) patients diagnosed with either polymyositis (PM), dermatomyositis (DM), or myositis associated with a connective tissue disease according to established diagnostic criteria ; and (3) myotonic dystrophy type 1 (DM1) who has characteristic grip and percussion myotonia and an expansion of the cytosine-thymine-guanine (CTG) triplet repeat in the myotonic dystrophy protein kinase gene. This study was approved by the Institutional Review Board of Tokushima University. The subjects provided written informed consent at the time of testing.

Sonography

A single technician (N.T.) blinded to patient diagnoses performed sonography using a LOGIQ7 (GE Healthcare Japan, Tokyo) with a fixed 11-MHz linear-array transducer. The subjects were tested in the supine position and the right lower limbs were studied. By applying the transducer to the medial aspect of the mid-calf, the medial head of gastrocnemius was identified (Figure 1). The images were saved as a bitmap format and assessed offline for the following texture analysis.

Texture analysis and machine learning

The calculation of texture features was performed by using the LIFEx program, version 3.36 (IMIV, CEA, France : https://www.

Abbreviations
DM = dermatomyositis, DM1 = myotonic dystrophy type 1, EI = echo-intensity, GLCM = gray level co-occurrence matrix, GLNU = gray-level non-uniformity, GLRLM = gray-level run length matrix, GLZLM = gray-level zone length matrix, IBM = inclusion body myositis, NGLDM = neighborhood gray-level different matrix, PM = polymyositis, ROI = region of interest, US = ultrasound

Received for publication January 11, 2019 ; accepted February 19, 2019.

Address correspondence and reprint requests to Hiroyuki Nodera, MD, Department of Neurology, 3-18-15 Kuramotocho, Tokushima City, 770-8503 Japan, and Fax : 81-88-633-7208.

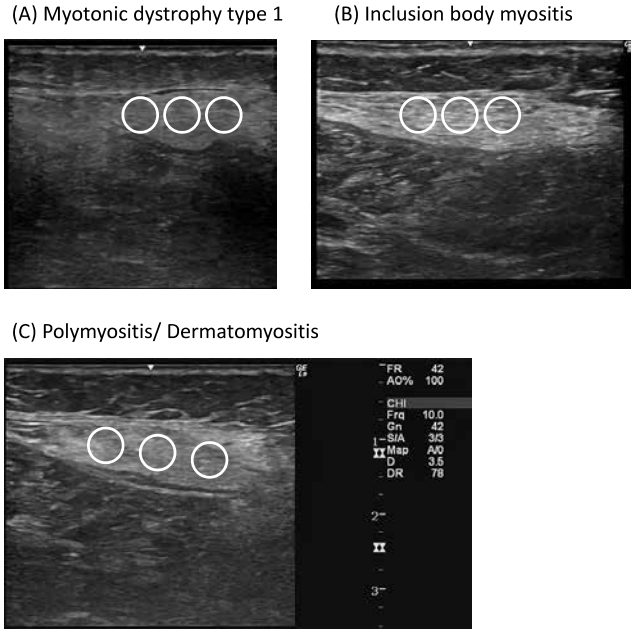

Figure 1 : Representative ultrasound images of the medial lower leg. The regions of interest (ROIs) are superimposed where texture calculation was performed.

lifexsoft.org/). Identical sizes of three circular-shaped regions of interest (ROI) were set to cover the largest area of the medial gastrocnemius muscle, but not to include the hyperechoic epimysium. The total ROI area was set at 4.0 cm^2. The LIFEx program yields 40 imaging features : the indices from histogram ; the gray level co-occurrence (GLCM) matrix [Haralick] ; the neighborhood gray-level different (NGLDM) matrix [Amadasum] ; the gray-level run length (GLRLM) matrix [Xu] ; the gray-level zone length (GLZLM) matrix [Thibault].

Classification was performed by WEKA machine learning software (version 3.8.0, The University of Waikato, New Zealand). The numeric values were normalized to have a range from 0-1. The following classifiers were used to classify the instance : (1) Simple Logistic, (2) SMO (support vector machine), and (3) Random Forest.

Percentages of classified instances were assessed by 10-fold validation (90% of the instances were used as training data and the rest of the 10% was used as the test data that are regarded as unrelated, new data to test the established model, whose process were repeated 10 times by selecting different portions and the averaged percentage was provided).

In order to identify useful texture attributes for classification, attribute selection was performed (Weka 3.8). The evaluator was ReliefFAttributeEval with the ranker search method. The top 5 attributes were selected.

Data analysis

EZR on R commander version 1.37 was used for statistical analysis, using the t-test and one-way ANOVA with Holm post-hoc test, where applicable. (4) A *P* value of 0.05 was set as the threshold for statistical significance.

RESULTS

Clinical characteristics

The subject characteristics are summarized in Table 1. As reported, the IBM patients were older than other two classes. Despite the different gender distribution (male dominance in IBM and female dominance in PM/DM), the gender ratio was not statistically significant.

Table 1: clinical characteristics of the subjects.

	IBM (A)	PM/DM (B)	DM1 (C)	*P* value
Number (men/women)	11 (7/4)	21 (6/15)	19 (9/10)	0.14
Age [mean ± SD ; (range)]	75.4 ± 6.6 (62 - 82)	63.1 ± 11.9 (39 - 81)	50.4 ± 10.6 (37 - 66)	< 0.01 (A vs B, B vs C, C vs A)

Sonography

Representative sonographic images are shown in Figure 1. As previously reported, IBM and DM1 showed preferential high echodensity regions in the medial gastrocnemius. (5,6) The representative view of LifeX texture analytic system is shown in Figure 2. Based on the calculated texture features as shown in the superimposed spreadsheet, the following analyses were performed. In Figure 3, comparisons of the texture features are shown among the three groups of the subjects. The mean pixel value (i.e., the greater the pixel value, the whiter the images) showed no statistical significance, although IBM tended to show greater values than the other two groups. By contrast, the maximum pixel value showed statistical significance between DM1 and other two groups, suggesting greater pixel variability in IBM and PM/DM than DM1. NGLDM_Coarseness [NGLDM = the neighborhood grey-level different matrix] also showed statistical significance. Figure 4 shows the comparison of the texture features when IBM and PM/DM were grouped together as inflammatory myopathy and compared with DM1. Similar to Figure 3, the mean pixel values were similar between IBM + PM/DM vs. DM1. However, the standard deviation of pixel values, histogram entropy, and the grey-level run length matrix (GLRLM) - gray-level non-uniformity (GLNU) all showed statistical significance.

Table 2 shows the result of classification by commonly used machine-learning algorithms. All three algorithms showed greater than 76% of classification accuracies, random forest being the top that reached 78.4% classification accuracy. In Table 3, similar classification was attempted among the three groups of subjects. Random forest showed 58.8% of accuracy, but overall classification was not satisfactory. Table 4 shows the selected texture attributes that were computed as useful for classification. The most useful attribute was the standard deviation of pixel value in the two- and three-groups analysis.

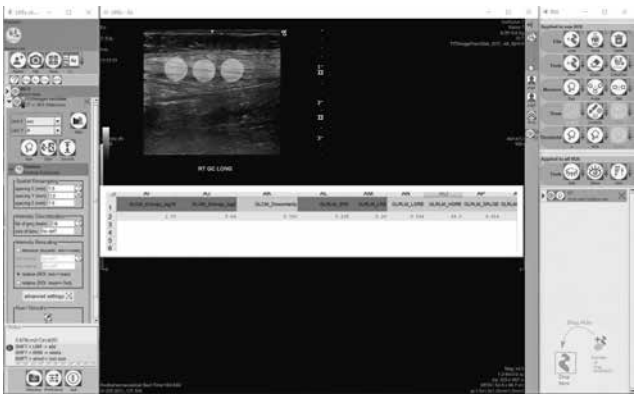

Figure 2 : A representative screenshot of the texture analytic software (LifeX). The calculated texture parameters are saved in a superimposed spreadsheet (the lower middle part).

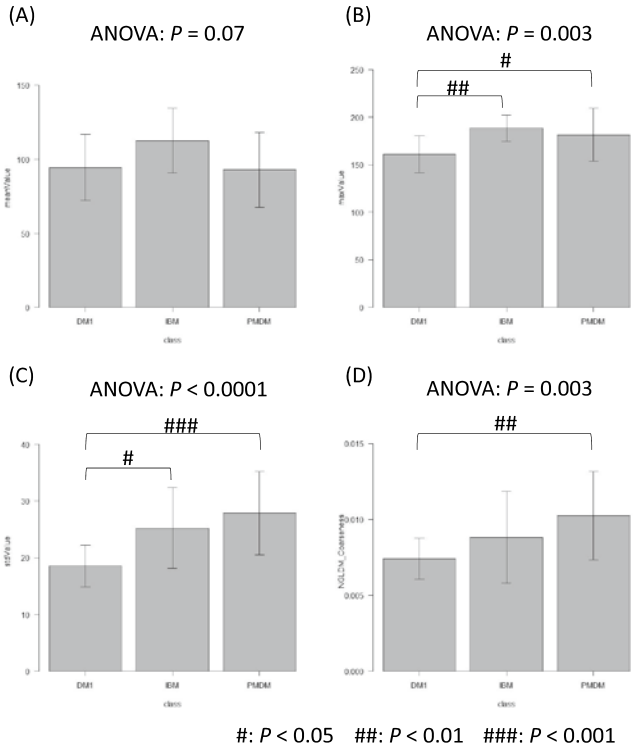

Figure 3 : Comparison of representative values of the three groups. Although the mean pixel values were not statistically significant (A), other values showed significance. B = maximum pixel value ; C = the standard deviation of pixel values ; D = NGLDM_Coarseness [NGLDM = the neighborhood grey-level different matrix]

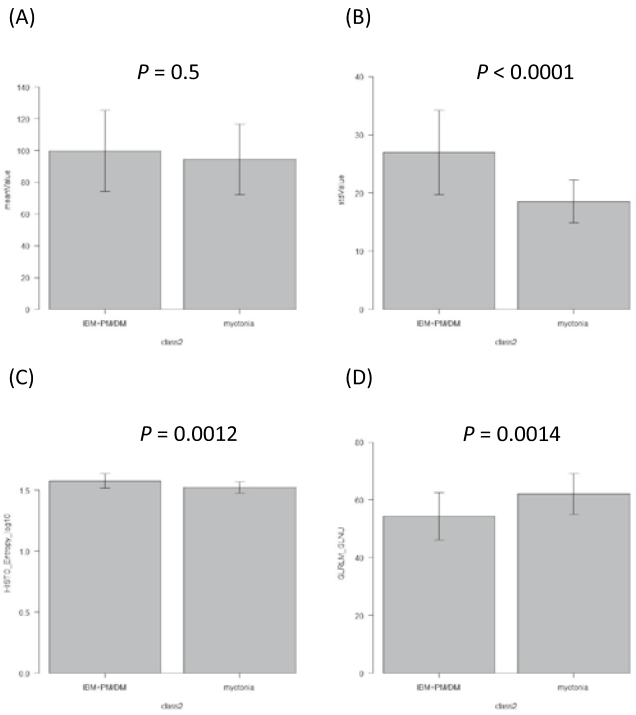

Figure 4 : Comparison of representative values of the two groups [inflammatory myopathy (IBM + PM/DM ; myotonic dystrophy type 1 (DM1)]. Similar to Figure 2, the mean pixel values were similar (A), but other values showed difference. B = the standard deviation of pixel values ; C = histogram entropy ; D = GLRLM = the grey-level run length matrix (GLRLM) - gray-level non-uniformity (GLNU)

Table 2 : Confusion matrices of classification between the two classes (inflammatory myopathy [IM] vs. myotonic dystrophy type 1 [DM1])

	IM (classified)	DM1 (classified)
IM (actual)	(26)	6
DM1 (actual)	6	(13)

(1) Simple Logistic (correctly classified instances : 76.5%)

	IM (classified)	DM1 (classified)
IM (actual)	(29)	3
DM1 (actual)	9	(10)

(2) SMO (support vector machine) (correctly classified instances : 76.5%)

	IM (classified)	DM1 (classified)
IM (actual)	(28)	4
DM1 (actual)	7	(12)

(3) Random Forest (correctly classified instances : 78.4%)

Table 3 : Confusion matrices of classification among the three classes (inclusion body myositis [IBM], polymyositis/dermatomyositis [PM/DM], and myotonic dystrophy type 1 [DM1])

	IBM (classified)	PM/DM (classified)	DM1 (classified)
IBM (actual)	(13)	1	5
PM/DM (actual)	5	(0)	6
DM1 (actual)	4	3	(14)

(1) Simple Logistic (correctly classified instances : 52.9%)

	IBM (classified)	PM/DM (classified)	DM1 (classified)
IBM (actual)	(15)	0	4
PM/DM (actual)	4	(10)	7
DM1 (actual)	5	3	(13)

(2) SMO (support vector machine) (correctly classified instances : 54.9%)

	IBM (classified)	PM/DM (classified)	DM1 (classified)
IBM (actual)	(16)	1	2
PM/DM (actual)	3	(2)	6
DM1 (actual)	5	4	(12)

(3) Random Forest (correctly classified instances : 58.8%)

Table 4 : Selection of texture attributes that were useful for classification. Evaluator = ReliefFAttributeEval, search method = ranker

2-class classification	3-class classification
1 : standard deviation of pixel value	1 : standard deviation of pixel value
2 : maximum pixel value	2 : maximum pixel value
3 : HISTO_Entropy_log10	3 : GLRLM_LRE
4 : HISTO_Entropy_log2	4 : GLRLM_RP
5 : GLRLM_GLNU	5 : NGLDM_Coarseness

HISTO = histogram [HISTO_Entropy reflects randomness of the distribution] ;
GLRLM = the grey-level run length matrix ;
LRE = long-run emphasis [GLRLM-LRE is the distribution of the long homogeneous runs in an image] ;
RP = run percentage [GLRLM-RP measures the homogeneity of the homogeneous runs] ;
GLNU = gray-level non-uniformity [GLRLM-GLNU is the non-uniformity of the gray-levels] ;
NGLDM = the neighborhood grey-level different matrix [NGLDM corresponds to the difference of grey-level between one voxel and its 8 neighbors. NGLDM_Coarseness is the level of spatial rate of change in intensity]

DISCUSSION

In this study, we performed texture analysis from ultrasound images and machine learning methodology in patients with three groups of myopathic conditions. Our study showed that the methodology classified DM1 vs. inflammatory myopathy. Variation of pixel intensity had the highest usefulness in our image set.

Texture analysis

Radiomics is an emerging translational field of imaging research aiming to extract high-dimensional data from clinical images. (7) Medical images are analyzed as digital information where quantitative calculation can be performed. Texture analysis, or texture features are one of such calculated features that represent coarseness or fineness of the particular portion. Texture analysis allows objective assessment of lesion and organ heterogeneity beyond what is possible with subjective visual interpretation and may reflect information about the tissue microenvironment. (8)

A number of imaging modalities have utilized texture analysis, including CT, MRI, PET, and ultrasound. (7) There have been some reports utilizing texture analysis in muscle ultrasound. Sogawa and colleagues recently showed that texture analysis can classify neurogenic and myogenic diseases. (3) Kumbhare, *et al*. successfully classified the patients with myofascial pain syndrome and healthy controls by texture analysis of trapezius muscle. (9) Matta and colleagues reported that texture analysis was a sensitive method to follow-up muscle damage. (10) Our data were in line of the previous reports and confirmed the usefulness of muscle texture analysis. The analysis was particularly useful in differentiating between DM1 and inflammatory myopathy in our dataset. This information is of potential significance because these two conditions require different therapies, particularly immune therapy. If categories of myopathic conditions can be inferred non-invasively, patients' need of muscle biopsy could be reduced by texture analysis, thus muscle texture analysis can be regarded as non-invasive muscle biopsy.

Study limitations

This study has several limitations. First, the number of the subjects are apparently small, thus widespread stages of the diseases were not covered. Second, we studied a single muscle. Other muscles that are more severely affected in respective myopathies might provide more useful data. Of note, however, we have reported that gastrocnemius is one of the most severely affected muscles in IBM and DM1, (5, 6) but obviously thigh and shoulder-girdle muscles should be more representative of abnormality in PM/DM.

CONFLICT OF INTEREST STATEMENT

None of the authors has conflict of interest.

FUNDING

This work was supported (in part) by Grants-in-Aid from the Research on Measures for Intractable Diseases and a Health and Labour Sciences Research Grant on Rare and Intractable Diseases (Evidence-based Early Diagnosis and Treatment Strategies for Neuroimmunological Diseases) from the Ministry of Health, Labour and Welfare of Japan. Also, this work was supported by JSPS KAKENHI Grant Number 17K09800.

REFERENCES

1. Szczypinski PM, Strzelecki M, Materka A, Klepaczko A. MaZda--a software package for image texture analysis. Comput Methods Programs Biomed 2009 ; 94 : 66-76.
2. Kassner A, Thornhill RE. Texture analysis : a review of neurologic MR imaging applications. AJNR Am J Neuroradiol 2010 ; 31 : 809-816.
3. Sogawa K, Nodera H, Takamatsu N, *et al*. Neurogenic and Myogenic Diseases : Quantitative Texture Analysis of Muscle US Data for Differentiation. Radiology 2017 ; 283 : 492-498.
4. Kanda Y. Investigation of the freely available easy-to-use software 'EZR' for medical statistics. Bone Marrow Transplant 2013 ; 48 : 452-458.
5. Nodera H, Takamatsu N, Matsui N, *et al*. Intramuscular dissociation of echogenicity in the triceps surae characterizes sporadic inclusion body myositis. Eur J Neurol 2016 ; 23 : 588-596.
6. Takamatsu N, Sogawa K, Nodera H, *et al*. Preferential changes of skeletal muscle echogenicity in myotonic dystrophy type 1. Eur J Neurol 2017 ; 24 : 366-373.
7. Rizzo S, Botta F, Raimondi S, *et al*. Radiomics : the facts and the challenges of image analysis. Eur Radiol Exp 2018 ; 2 : 36.
8. Lubner MG, Smith AD, Sandrasegaran K, Sahani DV, Pickhardt PJ. CT Texture Analysis : Definitions, Applications, Biologic Correlates, and Challenges. Radiographics 2017 ; 37 : 1483-1503.
9. Kumbhare D, Shaw S, Ahmed S, Noseworthy MD. Quantitative ultrasound of trapezius muscle involvement in myofascial pain : comparison of clinical and healthy population using texture analysis. J Ultrasound 2018.
10. Matta TTD, Pereira WCA, Radaelli R, Pinto RS, Oliveira LF. Texture analysis of ultrasound images is a sensitive method to follow-up muscle damage induced by eccentric exercise. Clin Physiol Funct Imaging 2018 ; 38 : 477-482.